Structure-Based Design and Synthesis of High Affinity Tripeptide Ligands of the Grb2-SH2 Domain

Pascal Furet,* Brigitte Gay, Giorgio Caravatti, Carlos García-Echeverría, Joseph Rahuel, Joseph Schoepfer, and Heinz Fretz*

Novartis Pharma Inc., Oncology Research Department, CH-4002 Basel, Switzerland

Received March 16, 1998

The X-ray structure of the Grb2-SH2 domain in complex with a specific phosphopeptide ligand has revealed the existence of an extended hydrophobic area adjacent to the primary binding site of the ligand on the SH2 domain. This has been exploited to design hydrophobic C-terminal groups that improve the binding affinity of the minimal sequence pTyr-Ile-Asn recognized by the Grb2-SH2 domain. The most significant increase in affinity (25-fold compared to that of the reference peptide having a nonsubstituted carboxamide C-terminus) was obtained with a 3-naphthalen-1-yl-propyl group which was predicted to have the largest contact area with the SH2 domain hydrophobic region. This modification combined with replacement of the minimal sequence isoleucine residue by 1-aminocyclohexane carboxylic acid to stabilize the β-turn conformation required for recognition by the Grb2-SH2 domain resulted in the high affinity (47 nM in an ELISA assay) and selective phosphopeptide Ac-pTyr-Ac_6c-Asn-NH(3-naphthalen-1-yl-propyl).

Introduction

Inhibition of the signal transduction pathways of tyrosine kinase growth factor receptors represents a novel approach under intensive investigation in cancer therapy research.[1−5] In particular, blocking the interaction between the phosphotyrosine (pTyr) containing-activated receptors and the *src* homology 2 (SH2) domain of the growth factor receptor-bound protein-2 (Grb2) constitutes an attractive strategy to develop new antitumor agents due to its potential to shut down the mitogenically important *ras* activation pathway.[6−8] Following this concept, we have engaged in a medicinal chemistry project aiming at the discovery of low molecular weight compounds that can efficiently disrupt these protein−protein interactions. The starting point for chemistry in the project was the minimal peptide sequence pTyr-Ile-Asn recognized by the Grb2-SH2 domain.[9] Previously, molecular modeling using the X-ray crystal structure of a SH2 domain homologue to that of Grb2 in the region of the phosphotyrosine binding pocket has allowed us to identify a N-terminal group that confers high affinity to this minimal sequence.[10] The recent determination of the structure of the Grb2-SH2 domain itself in complex with the phosphopeptide Lys-Pro-Phe-pTyr-Val-Asn-Val-NH2,[11] a sequence belonging to one of the endogenous protein ligands of Grb2, has strengthened the structural basis of our optimization efforts. The determinants of specificity for binding to the Grb2-SH2 domain have been revealed in full atomic details, opening new opportunities for structure-based design. In the present article, we report how this information has been used to enhance the binding affinity of the minimal sequence by attachment of lipophilic C-terminal groups designed to interact with a large hydrophobic area of the SH2 domain.

Design Rationale. A possible approach to increase the affinity of the minimal peptide sequence binding to a target protein consists of trying to create additional favorable contacts with the latter by appending N- or C- terminal groups to the sequence that exploit interactions outside the primary ligand binding site. We inspected the X-ray structure of the ligated Grb2-SH2 domain to identify interaction sites that could serve this purpose.

In the course of the analysis, the presence of an extended hydrophobic region on the surface of the SH2 domain, close to the location of the C-terminus of the bound phosphopeptide, was noticed. This is formed by the side chains of residues Leu-βD′1, Phe-βE3, and the hydrocarbon part of the side chain of Lys-βD6.[12] As shown in Figure 1, the side chain of the valine amino acid occupying the C-terminal position (pTyr+3)[13] of the phosphopeptide ligand in the X-ray structure points toward this hydrophobic area making van der Waals contacts with Leu-βD′1 and Lys-βD6.

This suggested that it should be possible to gain potency by attaching appropriate lipophilic groups to the C-terminus (pTyr+2 position) of the minimal sequence. The hydrophobic interactions formed by the pTyr+3 residue in the X-ray structure could thus be mimicked and even be made more extensive by taking advantage of the large size of the hydrophobic region identified on the Grb2-SH2 domain. Therefore, phosphopeptides of the form Ac-pTyr-Ile-Asn-NH−R were envisaged for synthesis. By constructing models of these molecules, it was shown that they were able to maintain the β-turn conformation adopted by the ligand in the X-ray structure (their C-terminal carboxamide function includes a NH group corresponding to the

* Corresponding authors. E-mail: pascal.furet@pharma.novartis.com or heinz.fretz@pharma.novartis.com.

S0022-2623(98)00159-9 CCC: $15.00
Published on Web 07/30/1998

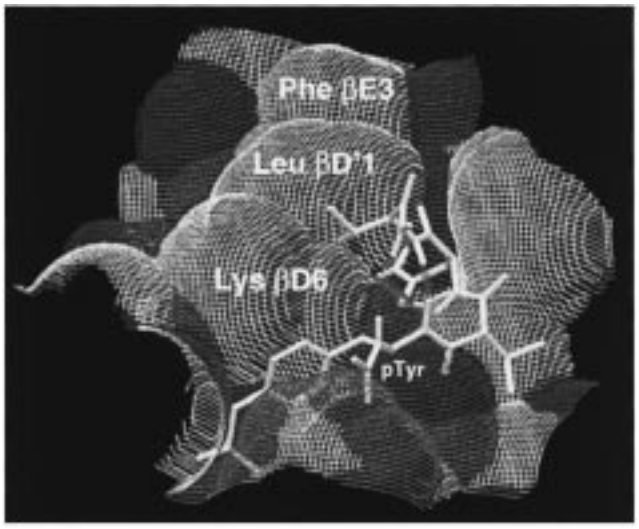

Figure 1. X-ray structure of phosphopeptide Lys-Pro-Phe-pTyr-Val-Asn-Val-NH_2 bound to the SH2 domain of Grb2. For clarity, the amino acids N-terminal to pTyr are not represented. The ligand binding site is represented in the form of a color coded Lee and Richards solvent accessible surface.[29] Yellow, red, and blue regions correspond respectively to hydrophobic (carbon or sulfur), hydrogen bond donor, and hydrogen bond acceptor atoms of the protein. Good van der Waals contacts between the ligand and the protein are established when the atoms of the former, represented in skeletal form, lie very close to the surface. The β-turn internal hydrogen bond formed between the backbone carbonyl of pTyr and the backbone NH of pTyr+3 is materialized as a dashed line.

backbone nitrogen atom of the pTyr+3 position which is involved in the β-turn internal hydrogen bond) while presenting the lipophilic R groups in a proper orientation to make favorable contacts with the hydrophobic area of the SH2 domain.

Different C-terminal hydrocarbon R groups were designed by molecular modeling with the objective of creating multiple van der Waals contacts with the amino acids forming the hydrophobic surface. We found that in order to create a first contact, aliphatic groups should comprise a chain of at least three carbon atoms. Additional contacts could then be obtained by increasing the length of the chain or by branching. Groups with a terminal aromatic moiety were also modeled. For these, it appeared that a spacer consisting of three methylene units was needed between the C-terminal carboxamide nitrogen and the aromatic moiety to ensure optimal hydrophobic contact of the latter with the SH2 domain. Shorter or longer spacers gave either steric clashes with the protein or no interaction at all. In particular we designed the 3-naphthalen-1-yl-propyl group which was considered especially promising due to the large surface of interaction of the naphthyl ring with the protein. The energy-minimized model of the resulting phosphopeptide in complex with the Grb2-SH2 domain is shown in Figure 2. In the model, each of the 10 carbon atoms of the naphthyl ring is within van der Waals interaction distance of at least one carbon atom belonging to the side chains of Leu-βD′1 or Lys-βD6 (distances between 3.4 and 4.0 Å). Less extensive contacts were obtained for aliphatic groups of reasonable size and for those terminated by a single phenyl ring.

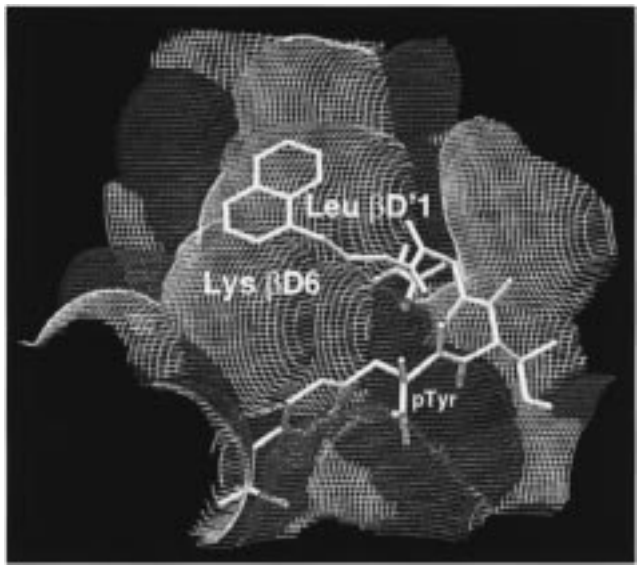

Figure 2. Model of the designed phosphopeptide **7** in complex with the Grb2-SH2 domain. The same type of representation as in Figure 1 is used. One can see that the atoms of the naphthyl moiety lie very close to the part of the surface corresponding to the side chains of Leu-βD′1 and Lys-βD6.

Chemistry

The peptide sequences Ac-pTyr-Ile-Asn-OAll and Ac-pTyr-Ac_6c-Asn-OAll were assembled using a semiautomated instrument on a Rink amide MBHA resin,[14] following standard Fmoc/*tert*-butyl chemistry protocol (Scheme 1).[15] All the couplings were done after preactivation of the Fmoc amino acids by means of TPTU.[16] In a first step, N^{α}-Fmoc-Asp-OAll was coupled through its side chain to the resin. On the basis of our previous studies concerning the synthesis of phosphotyrosine-containing peptides,[17] Fmoc-Tyr(PO_3Me_2)-OH was incorporated using the same method. A prolonged reaction time (6 h) was necessary for the complete coupling of Fmoc-Tyr(PO_3Me_2)-OH onto the Ac_6c residue. Generally, Fmoc cleavage was done with a solution of 20% piperidine in DMA. However, a solution of 2.5% of the nonnucleophilic base 1,8-diazabicyclo[5.4.0]undec-7-ene (DBU) in DMA turned out to be advantageous for Fmoc removal of Tyr(PO_3Me_2) containing peptides in order to minimize premature mono-demethylation of Tyr(PO_3Me_2).[18] The allyl ester was removed by treatment of a degassed chloroform solution of the peptide resin, containing acetic acid and *N*-methylmorpholine, with palladium(0) as catalyst.[19] The coupling of the amines (Chart 1) onto the C-terminal Asn residue was accomplished after preactivation of the resin with TPTU/HOBt.[16] Demethylation of the phosphate methyl groups was achieved with a 10-fold molar excess of TMSI in MeCN for 4 h at room temperature.[17b] After this time, we could demonstrate that the demethylation was complete with all the peptides investigated. Extensive washings with MeCN, MeOH, DMA and CH_2Cl_2 guaranteed the complete removal of excess reagents and soluble byproducts. Subsequent cleavage from the resin was accomplished with 95% TFA/5% water affording the crude peptides generally in good yields (>85%, based on the loading of the starting resin) and high quality. The HPLC traces of the peptides containing Ile (peptides **2**−**7**) displayed a major byproduct of 10−20%, whereas

Scheme 1[a]

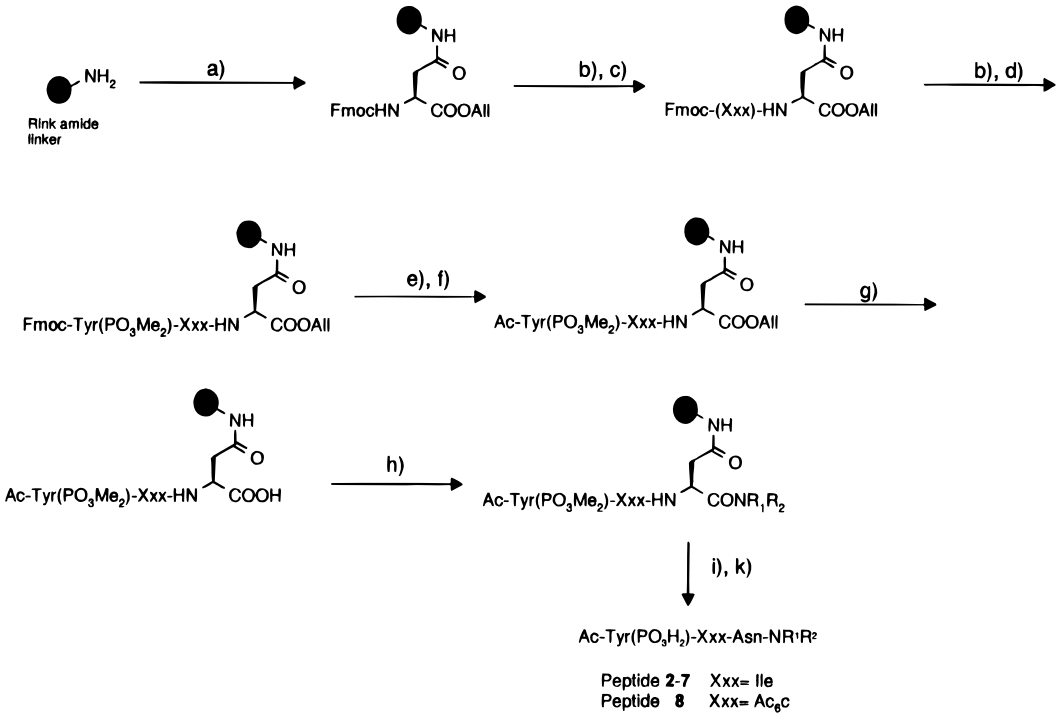

[a] Reagents and conditions (a) Fmoc-Asp-OAll, TPTU, DIEA; (b) 20% piperidine in DMA; (c) Fmoc-Ile-OH or FMoc-Ac_6c-OH, TPTU, DIEA; (d) Fmoc-Tyr(PO_3Me_2)-OH, TPTU, DIEA; (e) 2.5% DBU in DMA; (f) Ac_2O, pyridine; (g) $Pd(PPh_3)_4$, AcOH, NMM, $CHCl_3$; (h) preactivation with TPTU, HOBt, DIEA, then add amines; (i) TMSI, MeCN; (k) 95% TFA.

Chart 1[a]

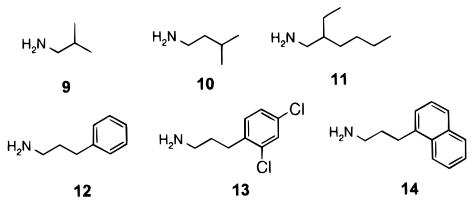

[a] Amines used for the C-terminal amidation. Amines **9**−**13** are commercially available. The synthesis of **14** is described in the Experimental Section.

mass spectrometrical analysis of the crude compounds revealed only the expected masses of the desired products. In fact, several side products can be expected. It is well-known from the literature that byproducts such as aspartimide, β-peptides, and piperidides can be formed under Fmoc cleavage conditions of Asp ester containing peptides.[20] In addition, partial racemization of Asn during the amidation step was expected since the C(α) center of C-terminally located amino acids in peptides is prone to racemization during activation of the C(α) carboxylic acid.[21] Identical masses for the main products as well as for the byproducts were measured after separation of the products by preparative MPLC. The pure peptides (>95%) were hydrolyzed (6 N HCl, 105 °C, 24 h), the hydrolysates were derivatized (*i*PrOH, 1.25 M HCl, 105 °C, 2 h; TFAA, CH_2Cl_2, 2 h, room temperature), and the cocktail of derivatized amino acids were analyzed by gas chromatography using a capillary column with a chiral stationary phase. In all of the cases, the main products consisted of L-amino acids and were assigned the desired peptides (**2**−**7**). The side products were found to be the corresponding epimers containing D-Asn. In addition, the structure of peptide **7** was unambiguously confirmed by ^1H, ^{31}P, and 2D NMR experiments at 20 °C and 120 °C ($^1H-^1H$ COSY, $^1H-^{13}C$ COSY, and HSQC, spectra not shown). Crude peptide **8** (single peak, >90%) was purified to homogeneity by preparative MPLC. Two sets of signals were observed in the ^1H NMR and ^{13}C NMR spectra integrating in a 87:13 ratio for a diastereomeric mixture. A sample of purified **8** was hydrolyzed, derivatized, and analyzed by GC as described above. The hydrolysate contained a 85:15 mixture of L- and D-Asn. Therefore, we concluded that the Ac_6c containing peptide **8** consists of the desired peptide **8** and its D-Asn epimer in a 85:15 ratio, which is fully consistent with the NMR data obtained.

Results and Discussion

The structures of phosphopeptides designed and synthesized as described in the above sections are reported in Table 1 together with their IC_{50} values in an ELISA-type assay that measures the ability of a compound to inhibit the binding of the phosphorylated C-terminal intracellular domain of the epidermal growth factor receptor (EGFR) to the Grb2-SH2 domain.

It can be seen in this table that our approach to increase the binding affinity of the mimimal peptide sequence was successful. As expected, the designed phosphopeptides inhibit the binding of the EGFR intracellular domain more potently than reference structure **1** whose C-terminal carboxamide function is not substituted. However, the magnitude of the effect is variable, depending on the nature of the C-terminal group. An isobutyl group (compound **2**),which exactly mimicks the side chain of the valine residue in pTyr+3 position of the X-ray structure ligand, improves the potency of **1** by a factor of 3. Although, modeling suggested that larger aliphatic moieties could make

Table 1. Inhibitory Activity of Phosphopeptides Ac-pTyr-X-Asn-NH−R to Grb2-SH2 in EGFR Assay

no.	X	R	IC_{50} (μM)[a]
1	Ile	H	8.9 ± 1.6
2	Ile		3.2 ± 0.2
3	Ile	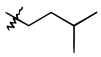	3.1 ± 0.3
4	Ile	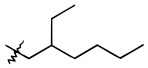	1.6 ± 0.4
5	Ile	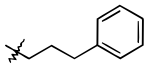	2.3 ± 0.1
6	Ile	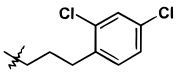	1.5 ± 0.1
7	Ile	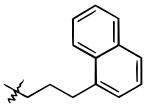	0.33 ± 0.02
8	Ac_6c	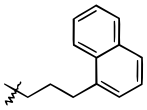	0.047 ± 0.001

[a] IC_{50} concentration to inhibit the binding of the phosphorylated C-terminal intracellular domain of EGFR to the Gbr2-SH2 domain.

more contacts with the hydrophobic region of the SH2 domain, compounds **3** and **4** bearing a 3-methyl-butyl and a 2-ethyl-hexyl group, respectively, are not significantly more active than **2**. The benefit of these additional contacts may have been lost by increasing conformational flexibility. In the design, we noticed that only specific conformations of the C-terminal groups gave rise to good hydrophobic interactions with the SH2 domain. Thus, very likely, there is an unfavorable decrease of their entropy upon binding, a phenomenon whose importance depends on the degree of conformational flexibility of the group. As far as the groups terminated with an aromatic moiety are concerned, the expected trend in activity is observed. Appending a single phenyl ring (compounds **5** and **6**) produces approximately a 5-fold increase of potency whereas the naphthyl analogue **7**, which was considered as the most promising synthetic target, is 25-fold more potent than **1**, an additional factor of 5 being gained. With an IC_{50} value of 0.33 μM, **7** represents a significant achievement in the optimization of the potency of the minimal peptide sequence by C-terminal modification.

Having this result in our hands, we envisaged further improvement of the binding affinity of the minimal sequence. This improvement could be accomplished by combining the attachment of the 3-naphthalen-1-yl-propyl C-terminal group with another previously identified beneficial structural modification. Combination with the 3-aminobenzyloxycarbonyl N-terminal group[10] was excluded due to the undesirable significant increase in molecular weight that would have resulted. Thus,

Table 2. Comparative IC_{50} of Phosphopeptides **7** and **8** To Block Various SH2 Domains

no.	SH2 domain	IC_{50} (μM)[b]
7	Grb2	0.58
7	$p56^{lck}$	>10
7	p85	>10
8	Grb2	0.064
8	$p56^{lck}$	>10
8	p85	>10

[b] IC_{50} concentration to inhibit the binding of a biotinylated phosphopeptide ligand specific to the SH2 domain.

8, the analogue of **7** in which the isoleucine pTyr+1 residue is replaced by 1-aminocyclohexyl carboxylic acid (Ac_6c), was synthesized. We have found that incorporation of this unnatural amino acid at the pTyr+1 position of the minimal sequence N-protected with the 3-aminobenzyloxycarbonyl group enhances potency.[22] The beneficial effect of this structural alteration is also observed here. Displaying an IC_{50} value of 47 nM, **8** is 1 order of magnitude more potent than **7** and therefore constitutes real progress in our medicinal chemistry program.

The specificity for the binding of phosphotyrosyl ligands by the Grb2-SH2 domain is determined by the presence of an asparagine residue in position pTyr+2 of the sequence.[23,24] However, we have recently shown that sequences of the pTyr-X-Asn type can also bind, though with low affinity (100 μM range), to other SH2 domains because the hydrogen bond interactions responsible for the recognition of the pTyr+2 asparagine by the Grb2-SH2 domain involve structural features that are conserved throughout the SH2 domains family.[25] It was therefore of interest to assess the consequences of the above structural modifications on selectivity. To this end, phosphopeptides **7** and **8** were tested in competition binding assays relative to two other SH2 domains (the N-terminal SH2 domain of the p85α subunit of phosphatidylinositol 3-kinase and the SH2 domain of $p56^{lck}$) besides that of Grb2. In these assays, the binding of a biotinylated phosphopeptide ligand specific to a given SH2 domain is challenged by the compound under study. The data reported in Table 2, clearly demonstrate that **7** and **8** bind selectively to the Grb2-SH2 domain. While in the Grb2-SH2 assay, the compounds show low IC_{50} values similar to those measured in the EGFR test, they do not inhibit the binding of the phospeptides specific to the other SH2 domains examined at concentrations of 10 μM.

Conclusion

Structure-based design in conjunction with the development of an appropriate synthetic strategy to incorporate C-terminal groups has allowed us to significantly improve the binding affinity of the minimal peptide sequence recognized by the SH2 domain of Grb2. With **8**, the most potent tripeptide resulting from this work, an improvement of 2 orders of magnitude was achieved. The low molecular weight of this compound associated with its high potency and selectivity represent an important step forward in our drug discovery program which aims at blocking a crucial protein−protein interaction in the signal transduction pathways of tyrosine kinase growth factor receptors.

Experimental Section

Abbreviations. The abbreviations for amino acids and the nomenclature of peptide structures follow the recommendations of the IUPAC-IUB Commission on Biochemical Nomenclature (*Eur. J. Biochem*. **1984**, *138*, 9). Other abbreviations are as follows: Ac_6c, 1-aminocyclohexyl carboxylic acid; DBU, 1,8-diazabicyclo[5.4.0]-undec-7-ene; DIEA, diisopropylethylamine; DMA, dimethylacetamide; Fmoc, 9-fluorenylmethoxycarbonyl; HPLC, high performance liquid chromatography; *i*PrOH, 2-propanol; MBHA, 4-methyl-benzhydrylamine; NMM, *N*-methylmorpholine; NMP, *N*-methyl-2-pyrrolidinone; NMR, nuclear magnetic resonance; TFA, trifluoroacetic acid; TMSI, trimethylsilyl iodide; TPTU, 2-(2-pyridon-1-yl)-1,1,3,3-tetramethyl-uroniumfluoroborate; t_R, retention time.

General. The synthesis of the peptide **1** was published previously.[10] All reagents were commercially available and were used without further purification. The amines **9**−**13** are commercially available from Fluka and Aldrich Chemical Co. Preparative flash chromatography was performed using Merck silica gel 60 (230−400 mesh). Medium-pressure liquid chromatography (MPLC) was done on a Büchi system, equipped with a Büchi 688 chromatography pump, a Büchi 687 gradient former, a Knauer variable wavelength monitor and a Büchi 684 fraction collector. The compounds were analyzed by reversed-phase HPLC using a Merck-Hitachi system, equipped with a AS-2000 autosampler, a L-6200A intelligent pump, a L-4500 diode array detector, and a D-6000 interface. NMR spectra of the compounds were measured in DMSO-d_6 solution on a Bruker Avance-500, at 300 K, with 500 MHz for ^{1}H NMR, 125.7 MHz for ^{13}C NMR, and 202.5 MHz for ^{31}P NMR experiments. All ^{1}H NMR spectra are reported in δ units, ppm downfield from tetramethylsilane using the residual solvent signal (δ 2.49 ppm for DMSO) as an internal standard. All ^{13}C NMR spectra are reported in ppm relative to the central line of the septet for DMSO at δ 39.5 ppm. Coupling constants (J) are reported in Hertz (Hz). Electrospray ionization mass spectra (ESI MS) were obtained with a Fisons Instruments VG Platform II. High-resolution mass spectra (HRMS) were recorded on a Micromass Quattro II instrument. Electrospray (negative ion mode) ionization method was applied with PEG 600 diacid as reference compound. Gas chromatography (GC) analyses were perfomed on a Varian 3600 gas chromatograph equipped with a FID.

3-(1-Naphthyl)-1-propylamine Hydrochloride (14). 1-Naphthaldehyde (7.8 g, 6.8 mL, 50 mmol) was placed in a flask equipped with a mechanical stirrer and a thermometer and was mixed with diethyl cyanomethylphosphonate (7.9 mL, 8.8 g, 0.04 mol) under N_2 atmosphere. A 6 M aqueous solution of K_2CO_3 (17 mL, 0.1 mol) was added dropwise to the vigorously stirred reaction mixture. During the addition, the temperature was kept at 20 °C by occasional cooling with an ice bath. The resulting mixture was stirred 15 min at room temperature, and then H_2O and ethyl acetate were added. The organic phase was separated, washed with water, dried (Na_2SO_4), and evaporated to give 3-(1-naphthyl)-acrylonitrile (10.4 g) as an oil in a 4:1 mixture of *E*/*Z* isomers.

This crude mixture (6.8 g, 37.9 mmol) was hydrogenated with Raney nickel (∼2 g) in MeOH (220 mL) containing 5% ammonia under 1 atm of H_2 at 45 °C (20 h). The catalyst was removed by filtration and the solvent evaporated. Flash chromatography of the yellow residue (ethyl acetate/MeOH, 9:1, containing 1% concentrated ammonia) gave the free base (5.3 g, 75% yield). The hydrochloride was obtained by dissolving the amine in ethanol (40 mL) and treating it with 10 mL of a 10% ethanolic HCl solution at 0 °C. Concentration of the resulting solution and addition of ether gave 3-(1-naphthyl)-1-propylamine hydrochloride **14** as colorless crystals (6.0 g, 73%): mp 154−156 °C; ^{1}H NMR (500 MHz, DMSO-d_6) δ 8.11 (d, J = 7.5 Hz, 1H), 8.03 (br s, 3H, N*H*$_3$), 7.92 (d, J = 7.5 Hz, 1H), 7.79 (d, J = 7.5 Hz, 1H), 7.55 (t, J = 7.5 Hz, 1H), 7.44 (t, J = 7.5 Hz, 1H), 7.39 (d, J = 7.5 Hz, 1H), 3.11 (t, J = 7.5 Hz, 2H, *H*-C(1)), 2.86 (t, J = 7.5 Hz, 2H, *H*-C(3)), 1.96 (tt, J = 7.5 Hz, 2H, *H*-C(2)); ^{13}C NMR (125.7 MHz, DMSO-d_6) δ 137.1, 133.5, and 131.2 (each 1 C_{quat}), 128.6, 126.7, 126.0, 125.9, 125.6, 125.6, and 123.8 (each 1C, *C*H, naphthyl), 38.6 (C(1)), 29.1, 28.1; ESI MS (positive ion mode) 186 $[M + H]^+$ calcd for $C_{13}H_{15}N$ 185.27.

Peptide Synthesis. The peptides were synthesized manually on a 4-(2′,4′,-dimethoxyphenyl-Fmoc-aminomethyl)-phenoxyacetamido-norleucyl-MBHA resin (Novabiochem, Läufelfingen, Switzerland, 0.55 mmol/g). Coupling was achieved by first dissolving the Fmoc-amino acid (3 equiv), DIEA (3.3 equiv), and TPTU (3 equiv, Senn Chemicals, Dielsdorf, Switzerland) in NMP, waiting 3 min for preactivation, adding the mixture to the resin, and finally shaking for at least 45 min. N^{α}-Fmoc-Asp-OAll is coupled through its side chain to the resin. The incorporation of N^{α}-Fmoc-Ile-OH, N^{α}-Fmoc-Ac_6c-OH, and N^{α}-Fmoc-Tyr(PO_3Me_2)-OH is accomplished with TPTU as described above. The coupling was complete after 1-h reaction time as checked by the Kaiser test, performed on the resin for the detection of free amino groups.[26] A prolonged reaction time of at least 6 h was required for complete condensation of N^{α}-Fmoc-Tyr(PO_3Me_2)-OH to the Ac_6c-containing sequence. Fmoc is removed with piperidine/DMA (1:4, v/v; 6 × 2 min) followed by washing with *i*PrOH (3 × 1 min), DMA (2 × 1 min), *i*PrOH (3 × 1 min), and DMA (2 × 1 min). The removal of the Fmoc group of the Tyr(PO_3Me_2)-containing peptide sequences was performed with 2.5% of the nonnucleophilic 1,8-diazabicyclo[5.4.0]undec-7-ene (DBU) in DMA for 10 min. An end-capping step with acetic anhydride/pyridine in DMA (1:1:8, v/v/v) for 2 min followed by washing with DMA and CH_2Cl_2 was included after each coupling cycle.

For the removal of the α-allyl ester, the dried peptide resin was resuspended in a degassed solution of acetic acid and NMM in $CHCl_3$ (2:1:37 v/v) followed by addition of tetrakis-(triphenylphosphine)-palladium(0) (0.8 equiv) under an argon atmosphere. After treatment for 3 h, the resin was washed with $CHCl_3$ (3 × 1 min), DMF (3 × 1 min), a solution of sodium diethyldithiocarbamate (0.05 M) containing 0.5% DIEA in DMF (2 × 1 min), DMF (2 × 1 min), and CH_2Cl_2 (3 × 1 min) and then dried.

The final incorporation of the amines was performed as follows: A sample of resin (200 mg) was subjected to preactivation conditions by means of TPTU/HOBt (1:1, 6 equiv) in the presence of DIEA (9 equiv) with NMP as solvent for 3 min. Then, a 10-fold excess of amine was added, and the resin was kept shaking for 2 h. The resin was rinsed with DMA and CH_2Cl_2 and dried.

For the cleavage of the phosphate methyl groups, dried Tyr(PO_3Me_2)-containing peptide resin was conditioned in MeCN and then treated with TMSI (10 equiv) in MeCN for 4 h.

The final peptide was cleaved from the resin by treatment with trifluoroacetic acid/H_2O (95:5, v/v) for 3 h at room temperature. The filtrate from the cleavage reaction was precipitated in diisopropyl ether/petroleum ether (1:1, v/v, 0 °C), and the precipitate was collected by centrifugation.

Purification of the Peptides. The crude peptides were purified by medium-pressure liquid chromatography using a reversed phase HPLC column material based on C_{18}-derivatized silica gel (Merck LICHROPREP RP-18, 15−25-μm bead diameter, Merck, Darmstadt, FRG) column length 46 cm, diameter 3.6 cm, flow rate 53.3 mL/min, detection at 215 nm. Elution was done with an MeCN−H_2O gradient containing 0.1% of TFA.

Analysis of the Peptides. The purity of the peptides was verified by analytical reversed-phase HPLC on a Nucleosil C_{18} column (250 × 4 mm, 5 μm (AB), 100 Å, Macherey-Nagel) with a linear gradient of H_2O/0.1% TFA (eluent A) and MeCN/0.09% TFA (eluent B) from 2 to 100% B (HPLC system A) and from 2 to 60% B (HPLC system B) over 20 min, flow rate 1.0 mL/min, detection at 215 nm.

HRMS revealed molecular masses within ±3 ppm of the expected values of the negative ion.

Determination of the D-Amino Acid Content. One milligram of the peptide was hydrolyzed in 1.0 mL 6 N HCl at 105 °C for 24 h. The hydrolysate was dried in vacuo over KOH at room temperature for 24 h. Derivatization was done

in a two-step procedure. First the dry residue was treated with 1.25 N HCl in 2-propanol (0.3 mL) at 105 °C for 2 h. The reaction mixture was dried in a stream of N_2. In a second step, the amino acid esters were *N*-acetylated with trifluoroacetic acid anhydride (TFAA, 0.2 mL) in CH_2Cl_2 (0.3 mL) for 2 h at room temperature. The volatiles were removed in a N_2 stream, and the residue was dissolved in ethyl acetate (1 mL). The mixture of derivatized amino acids was injected (1 mL) on a GC instrument equipped with a Chirasil valine capillary column at 75 °C. The amino acids eluted with a temperature gradient (6 min at 75 °C, then 75−180 °C with 4 °C/min).

Analytical data for acetyl-Tyr(PO_3H_2)-Ile-Asn-NH-isobutyl (2): HPLC single peak at t_R = 8.16 min (A), 10.67min (B, >95%); HRMS obs. 584.2462 [M − H]$^-$, calcd for $C_{25}H_{39}N_5O_9P$ 584.2486.

Acetyl-Tyr(PO_3H_2)-Ile-Asn-NH-(3-methyl-butyl) (3): HPLC single peak at t_R = 9.06 min (A), 12.17 min (B, >98%); HRMS obs. 598.2659 [M − H]$^-$, calcd for $C_{26}H_{41}N_5O_9P$ 598.2642.

Acetyl-Tyr(PO_3H_2)-Ile-Asn-NH-(2-ethyl-hexyl) (4): HPLC single peak at t_R = 11.27 min (A), 15.81 min (B, >98%); HRMS obs. 640.3101 [M − H]$^-$, calcd for $C_{29}H_{47}N_5O_9P$ 640.3112.

Acetyl-Tyr(PO_3H_2)-Ile-Asn-NH-(3-phenyl-propyl) (5): HPLC single peak at t_R = 9.88 min (A), 13.57 min (B, >98%); HRMS obs. 646.2623 [M − H]$^-$, calcd for $C_{30}H_{41}N_5O_9P$ 646.2642.

Acetyl-Tyr(PO_3H_2)-Ile-Asn-NH-[3-(2,4-dichloro-phenyl)-propyl] (6): HPLC single peak at t_R = 11.40 min (A), 16.09 min (B, >95%); HRMS obs. 714.1848 [M − H]$^-$, calcd for $C_{30}H_{39}Cl_2N_5O_9P$ 714.1863.

Acetyl-Tyr(PO_3H_2)-Ile-Asn-NH-(3-naphthalen-1-yl-propyl) (7): HPLC single peak at t_R = 11.03 min (A), 15.49 min (B, >95%); ^{1}H NMR (500 MHz, 300K, DMSO-d_6) δ 8.09 and 8.03 (each d, 2H, N$^\alpha$-*H*, Asn, pTyr), 8.05 (d, 1H, *H*-naphthyl), 7.97 (d, 1H, N$^\alpha$-*H*, Ile), 7.89 (d, 1 *H*-naphthyl), 7.89 (t, 1 H, N*H*-propyl), 7.74, 7.52 and 7.49 (each m, overlapping, 2 H, *H*-naphthyl), 7.39 (s, 1 H, N*H*$_2$−CO, Asn), 7.39 (m, 1H, *H*-naphthyl), 7.35 (d, 1H, *H*-naphthyl), 7.13 (d, 2H, *H*-phenyl, pTyr), 7.02 (d, 2H, *H*-phenyl, pTyr), 6.91 (s, 1H, N*H*$_2$−CO, Asn), 4.52 and 4.51 (each m, overlapping, 2H, *H*-C(α), Asn, *H*-C(α), pTyr), 4.14 (m, 1H, *H*-C(α), Ile), 3.14 (dd, 2H, C*H*$_2$), 3.01 (t, 2H, C*H*$_2$), 2.95 (dd, 1H, *H*-C(β), Asn), 2.67 (dd, 1H, *H*-C(β), Asn), 2.49 (m, 2H, *H*-C(β), pTyr), 1.78 (m, 2H), 1.75 (s, 3H, C*H*$_3$CONH), 1.71 (m, 2H, *H*-C(β), Ile), 1.41 (m, 1H, *H*-C(γ), Ile), 1.06 (m, 1H, *H*-C(γ), Ile), 0.81 (d, 3H, C*H*$_3$−C(β), Ile), 0.77 (t, 3H, *H*-C(δ), Ile); ^{13}C NMR (^{1}H−^{13}C COSY, DMSO-d_6) δ 129.6, 128.4, 126.1, 125.8, 125.5, 123.6, 119.3, 56.9, 53.5, 49.6, 38.2, 36.3, 36.1, 30.0, 29.3, 23.9, 22.1, 14.8, 10.5; ^{31}P NMR δ −4.53; HRMS obs. 696.2797 [M − H]$^-$, calcd for $C_{34}H_{43}N_5O_9P$ 696.2799.

Acetyl-Tyr(PO_3H_2)-Ac$_6$c-Asn-NH-(3-naphthalen-1-yl-propyl) (8): HPLC single peak at t_R = 10.86 min (A), 15.23 min (B, >98%); ^{1}H NMR (500 MHz, 300 K, DMSO-d_6) δ 8.19 (d, J = 7.5 Hz, 1H, *H*-naphthyl), 8.18 (s, 1H, N$^\alpha$-*H*), 8.08 (d, J = 7.0 Hz, 1H, N*H*), 7.92 (d, J = 7.5 Hz, 1H, *H*-naphthyl), 7.90−7.86 (m, 1H, N*H*-propyl), 7.76−7.71 (m, 1H, *H*-naphthyl), 7.52−7.45 (m, 2H, *H*-naphthyl, N*H*), 7.41−7.13 (m, 2H, *H*-naphthyl, CON*H*$_2$, Asn), 7.17 (d, J = 7.5 Hz, 2H, *H*-phenyl, pTyr), 7.02 (d, J = 7.5 Hz, 2H, *H*-phenyl, pTyr), 6.87 (s, 1H, CON*H*$_2$, Asn), 4.64 (m, 1H, *H*-C(α)), 4.35 (dd, J = 12 Hz, 5 Hz, 1H, *H*-C(α)), 3.20−3.12 (m, 2H, NC*H*$_2$), 3.02 (t, J = 7.5 Hz, 2H, *H*-C(3)), 3.00 (dd, J = 15 Hz, 5 Hz, 1H, *H*-C(β), Asn), 2.71 (dd, J = 15 Hz, 8 Hz, 1H, *H*-C(β), Asn), 2.61 (dd, J = 15 Hz, 7 Hz, 1H, *H*-C(β), pTyr), 2.53 (dd, J = 15 Hz, 4.5 Hz, 1H, *H*-C(β), pTyr), 1.99−1.10 (m, 10H, Ac$_6$c), 1.81 (m, 2H, C*H*$_2$), 1.78 (s, 3H, acetyl); ^{13}C NMR (125.7 MHz, DMSO-d_6, 300 K) δ 173.6, 172.8, 172.4, 170.5 and 170.0 (each 1 C, 5 *C*ONH), 138.1, 133.4 and 131.3 (each 1 C$_{quat}$, naphthyl), 129.9 and 129.8 (each 1 C(δ), pTyr), 128.5, 126.3, 125.9, 125.9, 125.6, 125.5, and 123.8 (each 1 C, 7 *C*H, naphthyl), 119.6 and 119.5 (each 1 C(ϵ), pTyr), 59.0 (1 C(α), Ac$_6$c), 54.3 (1 C(α), Asn), 50.3 (1 Ca, pTyr), 38.7 (NH*C*H$_2$), 35.8 and 35.4 (each 1 C(β), Asn, pTyr), 30.6 (2 *C*H$_2$, Ac$_6$c), 29.5 (2 *C*H$_2$, Ac$_6$c), 32.0, 24.8, and 20.6 (2 *C*H$_2$, propyl, 1 *C*H$_2$, Ac$_6$c), 22.3 (*C*H$_3$, acetyl); ^{31}P NMR (202 MHz, DMSO-d_6) δ −4.78; HRMS obs. 708.2788 [M − H]$^-$, calcd for $C_{35}H_{43}N_5O_9P$ 708.2799.

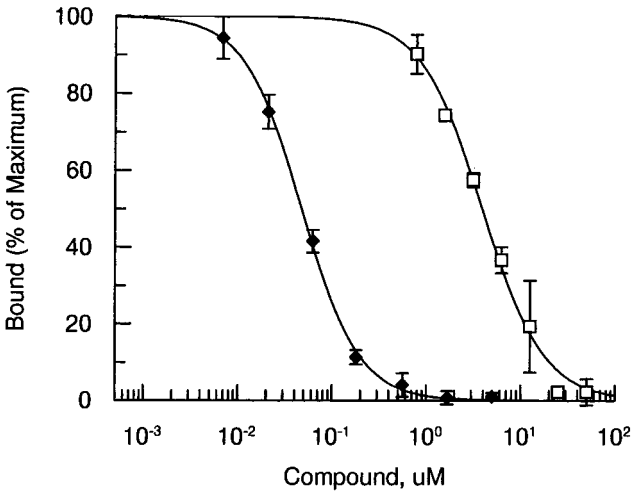

Figure 3. Inhibition curve of compound **8** in the EGFR assay (◆) and that of the Ac-EpYINQ-NH2 phosphopeptide, ED_{50} = 3.89 μM ± 0.21, as control (□).The standard deviation represents the mean of triplicates.

Cloning and Expression of Recombinant Proteins. Glutathione S-transferase (GST) fusion proteins of Grb2-(GST/Grb2-SH2), p56^{lck}-(GST/Lck-SH2)and p85-N-terminal-(GST/p85-N-SH2) SH2 domains were from Santa Cruz Biotech. The pMAL-c2 expression vector (New England Biolabs) was used to express the C-terminal domain of the epidermal growth factor receptor intracellular domain (residues 976−1210) as a maltose-binding fusion protein (MBP-EGFR) in *Escherichia coli* as already described.[11]

EGFR Assay. The assay has been described in detail previously.[11] Briefly, phosphorylated MBP-EGFR immobilized on a solid phase (polystyrene microtiter plates, NUNC MAXYSORB) was incubated with a GST/Grb2-SH2 fusion protein capable of binding to it, in the presence of a phosphopeptide in buffer or buffer alone. Bound SH2 was detected with polyclonal rabbit anti-GST antibody. Following washing, horseradish peroxidase-conjugated mouse antirabbit antibody was added. Peroxidase activity was monitored at 655 nm on a plate reader by adding 100 μL/well of a solution of tetramethylbenzidine as substrate.

Phosphopeptide Assays. This assay has already been described elsewhere.[27] A GST/SH2 domain fusion protein was paired, after buffer or varying concentrations of unlabeled phosphopeptides (as competitors) were added, with an appropriate high-affinity biotinylated phosphopeptide linked to streptavidin-coated microtiter plates. These biotinylated phosphopeptides are a subset of phosphotyrosyl peptides corresponding to SH2 targets on the EGFR, PDGFR, and Polyoma middle T antigen. A 100-μL portion of biotinylated phosphopeptide (10 ng/mL in 50 mM Tris, pH 7.5) was added to wells of streptavidin-coated plates (Boerhinger Mannheim), incubated overnight at 4 °C, and then rinsed with TBS. Selected peptide concentrations, or buffer alone, and GST/Grb2-SH2 (3.2 ng/mL), GST/Lck-SH2 (3.2 ng/mL), or GST/p85-N-SH2 (0.7 ng/mL) were then added to a 100 μL/well total volume of TBS buffer containing 0.1% Tween. The assay proceeded as described above for the MBP-EGFR assay with primary anti-GST antibody and secondary peroxidase-conjugated goat-antirabbit IgG.

Data Analysis. Peptide inhibition was calculated as a percentage of the reduction in absorbance in the presence of each peptide inhibitor concentration compared to the absorbance obtained with GST/SH2 in the absence of peptide inhibitor. Dose−response relationships were constructed by nonlinear regression of the competition curves with Grafit (Erithacus Software, London, U.K.). Fifty percent inhibitory concentrations (IC_{50}) were calculated from the regression lines (Figure 3).

Molecular Modeling. The modeling work was performed in MacroModel version 4.0[28] ("in house" version enhanced for

graphics by A. Dietrich, unpublished results). The C-terminal groups were designed interactively using a Lee and Richards solvent-accessible surface representation of the binding site (Bohacek and McMartin[29]) to guide the positioning of the groups such that they made good van der Waals contacts with the residues of the hydrophobic region of the Grb2-SH2 domain. Care was taken that the C-terminal groups were generated as conformational minima. Ligand-SH2 domain complexes corresponding to designed C-terminal groups making good van der Waals contacts with the protein (as judged from the close proximity of the group atoms in a skeletal representation to the solvent-accessible surface of the binding site) and presenting no apparent conformational strain were subjected to energy minimization to refine the models. The minimizations were performed using the AMBER force field[30] in conjunction with the GB/SA water solvation model.[31] The ligand as well as the protein residues within a distance of 5 Å were allowed to move freely upon energy minimization, while those at a distance between 5 and 8 Å were constrained by application of a parabolic force constant of 50 kJ/Å. Residues beyond 8 Å were ignored.

Acknowledgment. The authors are grateful to C. Stamm and M. G. D'Addio for their technical assistance, to Dr. J. Schneider for performing the NMR experiments, to Dr. C. Guenat for mass spectra, to G. Farrugio for amino acid analysis, and to R. Bohacek for providing the Lee and Richards solvent-accessible surface computer program.

References

(1) Alessandro, R.; Spoonster, J.; Wersto, R. P.; Kohn, E. C. Signal Transduction As a Therapeutic Target. *Curr. Top. Microbiol. Immunol*. **1996**, *213*, 167−188.

(2) Saltiel, A. R.; Sawyer, T. K. Targeting Signal Transduction in the Discovery of Antiproliferative Drugs. *Chem. Biol*. **1996**, *3*, 887−893.

(3) Gibbs, J. B.; Oliff, A. Pharmaceutical Research in Molecular Oncology. *Cell* **1994**, *79*, 193−198.

(4) Levitzki, A. Signal Transduction Therapy. A Novel Approach to Disease Management. *Eur. J. Biochem*. **1994**, *226*, 1−13.

(5) Traxler, P. Protein Tyrosine Kinase Inhibitors in Cancer Treatment. *Exp. Opin. Ther. Pat.* **1997**, *7*, 571−588.

(6) Gishizky, M. L. Tyrosine Kinase Induced Mitogenesis Breaking the Link with Cancer. In *Annual Reports in Medicinal Chemistry*; Bristol, J. A., Ed; Academic Press: San Diego, 1995; Vol. 30, pp 247−253.

(7) Smithgall, T. E. SH2 and SH3 Domains: Potential Targets for Anti-Cancer Drug Design. *J. Pharmacol. Toxicol. Methods* **1995**, *34*, 125−132.

(8) Beattie, J. SH2 Domain Protein Interaction and Possibilities for Pharmacological Intervention. *Cell. Signalling* **1996**, *2*, 75−86.

(9) Peptide studies have established that the minimal sequence retaining micromolar affinity for the Grb2-SH2 domain is the tripeptide pTyr-Ile-Asn. Asparagine at position pTyr+2 is absolutely required, while the pTyr+1 position is more versatile, valine, glutamine, and glutamic acid being good substitutes for isoleucine (Garcia-Echeverria, C.; et al. Novartis Pharma Inc., Oncology Research Department, unpublished results).

(10) Furet, P.; Gay, B.; Garcia-Echeverria, C.; Rahuel, J.; Fretz, H.; Schoepfer, J.; Caravatti, G. Discovery of 3-Aminobenzyloxycarbonyl as an N-Terminal Group Conferring High Affinity to the Minimal Phosphopeptide Sequence Recognized by the Grb2-SH2 Domain. *J. Med. Chem*. **1997**, *40*, 3551−3556.

(11) Rahuel, J.; Gay, B.; Erdmann, D., Strauss, A.; Garcia-Echeverria, C.; Furet, P.; Caravatti, G.; Fretz, H.; Schoepfer, J.; Gruetter, M. Structural Basis for Specificity of Grb2-SH2 Revealed by a Novel Ligand Binding Mode. *Nat. Struct. Biol.* **1996**, *3*, 586−589.

(12) For the nomenclature of the SH2 domain residues see: Lee, C. H.; Kominos, D.; Jacques, S.; Margolis, B.; Schlessinger, J.; Shoelson, S. E.; Kuriyan, J. Crystal Structures of Peptide Complexes of the Amino-Terminal SH2 Domain of the Syp Tyrosine Phosphatase. *Structure* **1994**, *2*, 423−438.

(13) Ligand residues are numbered relative to the position of the phosphotyrosine which is denoted pTyr0.

(14) Rink, H. Solid-phase synthesis of protected peptide fragments using a trialkoxy-diphenyl-methyl ester resin. *Tetrahedron Lett.* **1987**, *28*, 3787−3790.

(15) Atherton, E.; Sheppard, R. C. In Solid-Phase Peptide Synthesis - A Practical Approach, Rickwood, D., Hames, B. D., Eds.; IRL Press at Oxford University Press: Oxford, 1989.

(16) Knorr, R.; Trzeciak, A.; Bannwarth, W.; Gillessen, D. New Coupling Reagents in Peptide Synthesis. *Tetrahedron Lett.* **1989**, *30*, 1927−1930.

(17) (a) Fretz, H. N^{α}-Fmoc-*O*,*O*-(Dimethylphospho)-L-tyrosine Fluoride: A Convenient Building Block for The Solid-Phase Synthesis of Phosphotyrosyl Peptides. *Lett. Pept. Sci.* **1997**, *4*, 171−176. (b) Fretz, H. A. Practical Dealkylation Procedure for *O*,*O*-Dimethyl-phosphotyrosyl-containing Peptide-Resins. *Lett. Pept. Sci.* **1996**, *3*, 343−348. (c) Garcia-Echeverria, C. Evaluation of coupling conditions for the incorporation of N^{α}-Fmoc-Tyr(PO_3H_2)-OH in solid-phase peptide synthesis. *Lett. Pept. Sci.* **1996**, *2*, 369−373. (d) Garcia-Echeverria, C. Potential pyrophosphate formation upon use of Nα-Fmoc-Tyr(PO3H2)-OH in solid-phase peptide synthesis. *Lett. Pept. Sci*. **1995**, *2*, 93−98.

(18) Wade, J. D.; Bedford, J.; Sheppard, R. C.; Tregear, G. W. DBU as an Nα-deprotecting reagent for the fluorenylmethoxycarbonyl group in continuous flow solid-phase peptide synthesis. *Pept. Res.* **1991**, *4*, 194−199.

(19) (a) Albericio, F.; Barany, G.; Fields, G. B.; Hudson, D.; Kates, S. A.; Lyttle, M. H.; Sole, N. A. Allyl-based orthogonal solid-phase peptide synthesis. *Pept. 1992, Proc. Eur. Pept. Symp., 22nd*; Schneider, C. H., Eberle, A. N., Eds.; ESCOM: Leiden, The Netherlands, 1993; pp 191−193. (b) Kates, S. A.; Daniels, S. B.; Sole, N. A.; Barany, G.; Albericio, F. Automated allyl chemistry for solid-phase peptide synthesis: Applications to cyclic and branched peptides. *Pept.: Chem., Struct. Biol., Proc. Am. Pept. Symp., 13th*; Hodges, R. S., Smith, J. A., Eds.; ESCOM: Leiden, The Netherlands, 1994; pp 113−15.

(20) (a) Delforge, D.; Dieu, M.; Delaive, E.; Art, M.; Gillon, B.; Devreese, B.; Raes, M.; Van Beeumen, J.; Remacle, J. Solid-phase Synthesis of Tailed Cyclic Peptides: The Use of α-Allyl-protected Aspartic Acid Leads To Aspartimide and Tetramethylguanidinium Formation. *Lett. Pept. Sci.* **1996**, *3*, 89−07. (b) Karlström, A.; Undén, A. A New Protecting Group For Aspartic Acid That Minimizes Piperidine-Catalyzed Aspartimide Formation in Fmoc Solid Phase Peptide Synthesis. *Tetrahedron Lett.* **1996**, *37*, 4243−4246. (c) Packman, L. C. N-2-Hydroxy-4-Methoxybenzyl (Hmb) Backbone Protection Strategy Prevents Double Aspartimide Formation in a 'Difficult' Peptide Seqence. *Tetrahedron Lett.* **1995**, *36*, 7523−7526. (d) Yang, Y.; Seeney, W. V.; Schneider, K.; Thörnqvist, S.; Chait, B. T.; Tam, J. P. Aspartimide Formation in Base-driven 9-Fluorenylmethoxycarbonyl Chemistry. *Tetrahedron Lett.* **1994**, *35*, 9689−9692.

(21) (a) Spatola, A. F.; Darlak, K.; Romanovskis, P. An Approach to Cyclic Peptide Libraries: Reducing Epimerisation in Medium Sized Rings During Solid Phase Synthesis. *Tetrahedron Lett.* **1996**, *37*, 591−594. (b) Griehl, C.; Kolbe, A.; Merkel, S. Quantitative description of epimerization pathways using the carbodiimide method in the synthesis of peptides. *J. Chem. Soc., Perkin Trans. 2* **1996**, 2525−2529. (c) Valero, M.-L.; Giralt, E.; Andreu, D. Solid phase-mediated cyclization of head-to-tail peptides: problems associated with side chain anchoring. *Tetrahedron Lett.* **1996**, 37, 4229−4232. (d) Quibell, M.; Packman, L. C.; Johnson, T. Identification of coupling conditions proceeding with low C-terminal epimerization during the assembly of fully protected backbone-substituted peptide segments. *J. Chem. Soc., Perkin Trans. 1* **1996**, 1219−1225. (e) Somlai, C.; Szokan, G.; Penke, B. Epimerization-free amidation of protected peptide acids. *Synthesis* **1995**, 638−646. (f) Benoiton, N. L.; Lee, Y. C.; Chen, F. M. F. A new coupling method allowing epimerization-free aminolysis of segments: Use of succinimidyl esters obtained through mixed anhydrides. *Pept. 1994, Proc. Eur. Pept. Symp., 23rd*; Maia, H. L. S., Ed.; ESCOM: Leiden, The Netherlands, 1995; pp 203−204.

(22) Garcia-Echeverria, C.; Furet, P.; Gay, B.; Fretz, H.; Rahuel, J.; Schoepfer, J.; Caravatti, G. Potent Antagonists of the SH2 Domain of Gbr2: Optimization of the X_{+1} position of 3-amino-Z-Tyr(PO_3H_2)-X_{+1}-Asn-NH_2. *J. Med. Chem*. **1998**, *41*, 1741−1744.

(23) Songyang, Z.; Shoelson, S. E.; McGlade, J.; Olivier, P.; Pawson, T.; Bustelo, X. R.; Barbacid, M.; Sabe, H.; Hanafusa, H.; Yi. T.; Ren, R.; Baltimore, D.; Ratnofsky, S.; Feldman, R. A.; Cantley, L. C. Specific Motifs Recognized by the SH2 Domains of Csk, 3BP2, fps/fes, GRB-2, HCP, SHC, Syk and Vav. *Mol. Cell. Biol.* **1994**, *14*, 2777−2785.

(24) Songyang, Z.; Shoelson, S. E.; Chaudhuri, M.; Gish, G.; Pawson, T.; Hase, W. G.; King, F.; Roberts, T.; Ratnofsky, S.; Lechleider, R. J.; Neel, B. G.; Birge, R. B.; Fajardo, J. E.; Chou, M. M.; Hanafusa, H.; Schaffhausen, B.; Cantley, L. C. SH2 Domains Recognize Specific Phosphopeptide Sequences. *Cell* **1993**, *72*, 767−778.

(25) Gay, B.; Furet, P.; Garcia-Echeverria, C.; Rahuel, J.; Chêne, P.; Fretz, H.; Schoepfer, J.; Caravatti, J. Dual Specificity of Src Homology 2 Domains for Phosphotyrosine Peptide Ligands. *Biochemistry* **1997**, *36*, 5712−5718.

(26) Kaiser, E.; Colescott, R. L.; Bossinger, C. D.; Cook, P. I. Color test for detection of free terminal amino groups in the solid-phase synthesis of peptides. *Anal. Biochem*. **1970**, *34*, 595−598.

(27) García-Echeverría, C.; Stamm, C.; Wille, R.; Arz, D.; Gay, B. Biotinylated Phosphotyrosine Peptides: A Valuable Tool for Studies on Phosphopeptide Interactions with SH2 and PTB Domains. *Lett. Pept. Sci.* **1997**, *4*, 49−53.
(28) Mohamadi, F.; Richards, N. G.; Guida, W. C.; Liskamp, R.; Lipton, M.; Caufield, C.; Chang, G.; Hendrickson, T.; Still, W. C. Macromodel - An Integrated Software System for Modeling Organic and Bioorganic Molecules Using Molecular Mechanics. *J. Comput. Chem.* **1990**, *11*, 440−467.
(29) Bohacek, R. S.; McMartin, C. Definition and Display of Steric, Hydrophobic, and Hydrogen-Bonding Properties of Ligand Binding Sites in Proteins Using Lee and Richards Accessible Surface: Validation of High-Resolution Graphical Tool for Drug Design. *J. Med. Chem.* **1992**, *35*, 1671−1684.
(30) Weiner, S. J.; Kollman, P.; Case, D. A.; Singh, U. C.; Ghio, C.; Alagona, S.; Profeta, S.; Weiner, P. A Force Field for the Simulation of Nucleic Acids and Proteins. *J. Am. Chem. Soc.* **1984**, *106*, 765−770.
(31) Still, W. C.; Tempczyk, A.; Hawley, R. C.; Hendrickson, T. Semianalytical Treatment of Solvation for Molecular Mechanics and Dynamics. *J. Am. Chem. Soc.* **1990**, *112*, 6127−6129.

JM980159A